The EMBO Journal (2007) 26, 1602–1614 | © 2007 European Molecular Biology Organization | All Rights Reserved 0261-4189/07
www.embojournal.org

THE EMBO JOURNAL

N- and C-terminal residues of eIF1A have opposing effects on the fidelity of start codon selection

Christie A Fekete[1,3], Sarah F Mitchell[2,3], Vera A Cherkasova[1], Drew Applefield[2], Mikkel A Algire[2], David Maag[2], Adesh K Saini[1], Jon R Lorsch[2,*] and Alan G Hinnebusch[1,*]

[1]Laboratory of Gene Regulation and Development, National Institute of Child Health and Human Development, NIH, Bethesda, MD, USA and [2]Department of Biophysics and Biophysical Chemistry, Johns Hopkins University School of Medicine, Baltimore MD, USA

Translation initiation factor eIF1A stimulates preinitiation complex (PIC) assembly and scanning, but the molecular mechanisms of its functions are not understood. We show that the *F131A,F133A* mutation in the C-terminal tail (CTT) of eIF1A impairs recruitment of the eIF2-GTP-Met-tRNA$_i^{Met}$ ternary complex to 40S subunits, eliminating functional coupling with eIF1. Mutating residues 17–21 in the N-terminal tail (NTT) of eIF1A also reduces PIC assembly, but in a manner rescued by eIF1. Interestingly, the *131,133* CTT mutation enhances initiation at UUG codons (Sui$^-$ phenotype) and decreases leaky scanning at AUG, while the NTT mutation *17–21* suppresses the Sui$^-$ phenotypes of eIF5 and eIF2β mutations and increases leaky scanning. These findings and the opposite effects of the mutations on eIF1A binding to reconstituted PICs suggest that the NTT mutations promote an open, scanning-conducive conformation of the PIC, whereas the CTT mutations *131,133* have the reverse effect. We conclude that tight binding of eIF1A to the PIC is an important determinant of AUG selection and is modulated in opposite directions by residues in the NTT and CTT of eIF1A.

The EMBO Journal (2007) **26,** 1602–1614. doi:10.1038/sj.emboj.7601613; Published online 1 March 2007
Subject Categories: RNA; proteins
Keywords: eIF1A; *GCN4*; initiation; *Saccharomyces*; translation

Introduction

Decoding the AUG start codon in mRNA by methionyl-initiator tRNA (Met-tRNA$_i^{Met}$) and the ribosome is stimulated by an array of eukaryotic translation initiation factors (eIFs). The Met-tRNA$_i^{Met}$ is delivered to the 40S subunit in a ternary complex (TC) with the GTP-bound form of eIF2, forming the 43S PIC, in a process stimulated by eIF1, eIF1A, eIF3, and eIF5 (Hershey and Merrick, 2000; Hinnebusch, 2000; Asano *et al*, 2001b; Algire *et al*, 2002; Majumdar *et al*, 2003; Kolupaeva *et al*, 2005). In budding yeast, a web of interactions links eIFs 1, 3, 5, and the TC in a multifactor complex (MFC) whose formation promotes PIC assembly *in vivo* (Asano *et al*, 2001a; Valášek *et al*, 2002; Valasek *et al*, 2004; Singh *et al*, 2004; Jivotovskaya *et al*, 2006). The 40S binding of eIF1 also is stimulated by eIF1A (Maag and Lorsch, 2003; Majumdar *et al*, 2003) and the C -termini of these two factors are in close proximity in the 43S PIC (Maag *et al*, 2005), with eIF1A likely occupying the 'A' site (Battiste *et al*, 2000) and eIF1 bound near the 'P' site on the 40S subunit (Lomakin *et al*, 2003), the site of decoding during initiation.

The 43S PIC is recruited to the 5′ end of the mRNA and the AUG codon is selected as the PIC scans the leader, with the anticodon of Met-tRNA$_i^{Met}$ inspecting successive triplets in the P-site (Hershey and Merrick, 2000). In a reconstituted mammalian system, eIF1 and eIF1A promote scanning and formation of a 48S initiation complex (IC) at the start codon (Pestova *et al*, 1998), and the absence of eIF1 allows selection of non-AUG triplets (Pestova and Kolupaeva, 2002). This fits with genetic studies in yeast that identified mutations in eIF1 (encoded by *SUI1*) that increase initiation at a UUG at the 5′ end of the *HIS4* gene, suppressing mutations in the AUG codon (Sui$^-$ phenotype) (Donahue, 2000). It is thought that eIF1 promotes an open conformation of the PIC conducive to scanning and restricts base pairing of Met-tRNA$_i^{Met}$ with non-AUGs in the P-site (Lomakin *et al*, 2003).

Our analysis of a reconstituted yeast system revealed that GTP bound to eIF2 is partially hydrolyzed in 48S PICs, dependent on eIF5, but the P_i is not released from eIF2-GDP-P_i when a non-AUG triplet occupies the P-site. Base pairing of Met-tRNA$_i^{Met}$ with AUG triggers a conformational change wherein eIF1 and eIF1A move apart and eIF1 is released from its 40S binding site in the initiation complex. It appears that dissociation of eIF1 permits release of P_i from eIF2-GDP-P_i to finalize selection of the start codon (Algire *et al*, 2005; Maag *et al*, 2005). By contrast, AUG recognition elicits tighter binding of eIF1A to the complex, dependent on eIF5. A dominant Sui$^-$ mutation in eIF5 (*SUI5*) strengthens eIF1A binding with UUG in the P-site, correlating with increased initiation at UUG codons in *SUI5* cells *in vivo*. A similar finding was made for an eIF1A mutant lacking the ~50-residue unstructured CTT of eIF1A (*tif11-ΔC*, or just Δ*C*), which also confers a Sui$^-$ phenotype. It was proposed that the eIF1A CTT promotes formation of an open, scanning-conducive conformation of the PIC, and on AUG recognition, eIF5 antagonizes the eIF1A CTT, strengthening eIF1A's interactions and promoting a more closed conformation (Maag *et al*, 2006).

Translation of *GCN4* mRNA is a sensitive indicator of defects in TC recruitment *in vivo*. *GCN4* is repressed in

*Corresponding authors. Jon R Lorsch, Department of Biophysics and Biophysical Chemistry, Johns Hopkins University School of Medicine, 725 N. Wolfe St, 625 WBSB, Baltimore, MD 21205, USA.
Tel.: +1 (410) 955 3012; Fax: +1 (410) 955 0637;
E-mail: jlorsch@jhmi.edu or Alan G Hinnebusch, Laboratory of Gene Regulation and Development, National Institute of Child Health and Human Development, NIH, Building 6A/Room B1A-13, Bethesda, MD 20892, USA. Tel.: +1 (301) 496 4480; Fax: +1 (301) 496-6828;
E-mail: ahinnebusch@nih.gov
[3]These authors contributed equally to this work

Received: 4 October 2006; accepted: 22 January 2007; published online: 1 March 2007

amino acid-replete cells by upstream open reading frames (uORFs) in the 5′UTR. After translating uORF1, 40S subunits resume scanning and reinitiate translation at uORFs 2, 3 or 4, after which they dissociate from the mRNA and leave the *GCN4* ORF untranslated. *GCN4* translation is derepressed in amino acid-starved cells by phosphorylation of the α-subunit of eIF2 by kinase GCN2, which inhibits recycling of eIF2-GDP to eIF2-GTP. The ensuing reduction in TC concentration allows 40S subunits that translate uORF1 and resume scanning to bypass uORFs 2–4 and reinitiate downstream at *GCN4*. In nonstarved wild-type (WT) or *gcn2*Δ cells, by contrast, the high level of TC ensures that all 40S subunits scanning downstream from uORF1 quickly rebind TC, reinitiate at uORFs 2, 3 or 4, and dissociate from the mRNA without translating *GCN4* (Hinnebusch, 2005). We found previously that the Δ*C* truncation of the eIF1A CTT conferred constitutive derepression of *GCN4* translation in *gcn2*Δ cells. This Gcd$^-$ phenotype suggests that Δ*C* reduces the rate of TC binding to 40S subunits scanning downstream from uORF1, allowing a fraction to bypass uORFs 2–4 and reinitiate at *GCN4* (Olsen *et al*, 2003). Supporting this interpretation, Δ*C* reduces TC binding to 40S subunits in both native and reconstituted PICs (Fekete *et al*, 2005).

In this report, we provide new evidence supporting the dual role of the eIF1A CTT in TC recruitment and AUG selection, and pinpoint specific residues, Phe131 and Phe133, involved in both functions. We show that residues in the unstructured eIF1A NTT also affect PIC assembly *in vivo*, but through a distinct mechanism. Remarkably, mutations in the eIF1A NTT disrupt AUG selection in a manner opposite to that of the Δ*C* and *SUI5* mutations, exhibiting a hyperaccurate phenotype. A concordance of genetic and biochemical data indicates that interaction of eIF1A with the initiation complex is a determinant of start codon selection that is modulated by the unstructured tails of eIF1A.

Results

Mutation of F131 and F133 in the CTT impairs PIC assembly

Previously, we showed that the Δ*C* truncation of eIF1A residues 108–153 confers a Gcd$^-$ phenotype and reduces native 43S PIC levels *in vivo*. Ala substitutions of CTT residues 128–132 ($_{128}$DVNFE$_{132}$) and 133–137 ($_{133}$FGNAD$_{137}$) also produce Gcd$^-$ phenotypes, as does the mutation *F131A, F133A* (henceforth *131,133*) of the two Phe residues in these intervals. As substitutions of surrounding CTT residues 118–122, 123–127, 138–142, 143–148, and 149–153 did not confer Gcd$^-$ phenotypes (Fekete *et al*, 2005), it appeared that F131 and F133 play key roles in TC recruitment; hence, we set out to characterize the effects of the *131,133* mutation on 43S PIC assembly.

This and other eIF1A mutations described below were made in the *TIF11-FL* allele (tagged at the 5′ end with FLAG epitope) and introduced into a *tif11*Δ *gcn2*Δ strain by plasmid shuffling (Fekete *et al*, 2005). The *131,133* mutation produces a slow-growth (Slg$^-$) phenotype on complete (SC) medium (Figure 1A) and decreased polysome content (Figure 1B), without reducing eIF1A expression (Fekete *et al*, 2005). The *131,133* mutation also restores growth on medium containing the inhibitor of histidine biosynthesis 3-aminotriazole (3AT), and this 3AT-resistant (3AT^R) phenotype was diminished by a high-copy (hc) plasmid encoding the three subunits of eIF2 and tRNA$_i^{Met}$, comprising the TC (hc-TC) (Figure 1A). Gcd$^-$ mutations that derepress *GCN4* translation independent of eIF2α phosphorylation by GCN2 derepress histidine biosynthetic genes under GCN4 control and overcome the 3-AT-sensitive (3-AT^S) phenotype of *gcn2*Δ cells. Suppression of the 3AT^R/Gcd$^-$ phenotype of the *131,133* mutant by hc-TC suggests that it results, at least partly, from a reduced rate of TC loading on 40S subunits scanning downstream from uORF1, allowing a fraction to bypass uORFs 2–4 and reinitiate at *GCN4*. Increasing the TC concentration with hc-TC is thought to boost the rate of TC loading by mass action.

In a *GCN2*$^+$ strain, the *131,133* mutation led to ~six-fold derepression of a *GCN4-lacZ* reporter containing all four uORFs under non-starvation conditions compared with the ~15-fold induction of this reporter on starvation of the *TIF11*$^+$ strain for isoleucine and valine (Figure 1C). This indicates that *131,133* confers partial derepression of *GCN4* translation, confirming its Gcd$^-$ phenotype.

Biochemical evidence that the *131,133* mutation impairs TC recruitment came first from our finding that it reduces eIF2 binding to 40S subunits in native PICs stabilized by formaldehyde crosslinking of living cells. The 40S binding of eIF5 was also reduced, whereas the mutant eIF1A protein showed higher than WT levels in the 40S fractions commensurate with the increased level of 40S protein RPS2 (Figure 1D–E). (As previously observed (Valasek *et al*, 2004; Fekete *et al*, 2005), the 40S binding defect of eIF2 and eIF5 in the mutant is associated with increased degradation of these factors during centrifugation.) Considering that the amount of free 40S subunits was elevated in the mutant, the approximately equal amounts of eIF3 in the mutant and WT 40S fractions suggest that eIF3 recruitment also is reduced by *131,133* (Figure 1D–E). Thus, *131,133* impairs 40S binding of three different MFC components *in vivo*. (No reduction in 40S-bound eIF1 was apparent; however, eIF1 expression is elevated in this mutant (Supplementary Figure S1), making it difficult to assess the efficiency of eIF1 binding.)

We further demonstrated that *131,133* impairs the rate of TC loading on 40S subunits *in vitro* in reactions containing eIF1 and mRNA. Interestingly, the *131,133* mutation reduced the rate of TC binding in the presence of eIF1 by >six-fold, but had no effect in the absence of eIF1 (Figure 2A–B), eliminating the stimulatory effect of eIF1 on TC loading (Figure 2B). The *131,133* mutation also reduces the rate of TC loading ~four-fold in reactions lacking mRNA (0.009 ± 0.003 versus 0.042 ± 0.012 min^{-1}; data not shown). To determine whether the defect in TC loading could arise from defective 40S binding of the *131,133* protein, we measured the K_d of eIF1A for 40S subunits in the presence and absence of eIF1 (Figure 2C–E), and new in the presence of both eIF1 and TC (Figure 2E). The *131,133* mutation does not weaken interaction of eIF1A with 40S subunits under any of these circumstances. Hence, *131,133* impairs the function of eIF1A bound to 40S subunits in accelerating TC loading.

Mutations in the eIF1A NTT impair PIC assembly in a manner rescued by eIF1

To address the function of the NTT, we analyzed the phenotypes of Ala substitutions made in consecutive blocks of five amino acids of the *TIF11-FL* allele. Mutations of residues 7–11

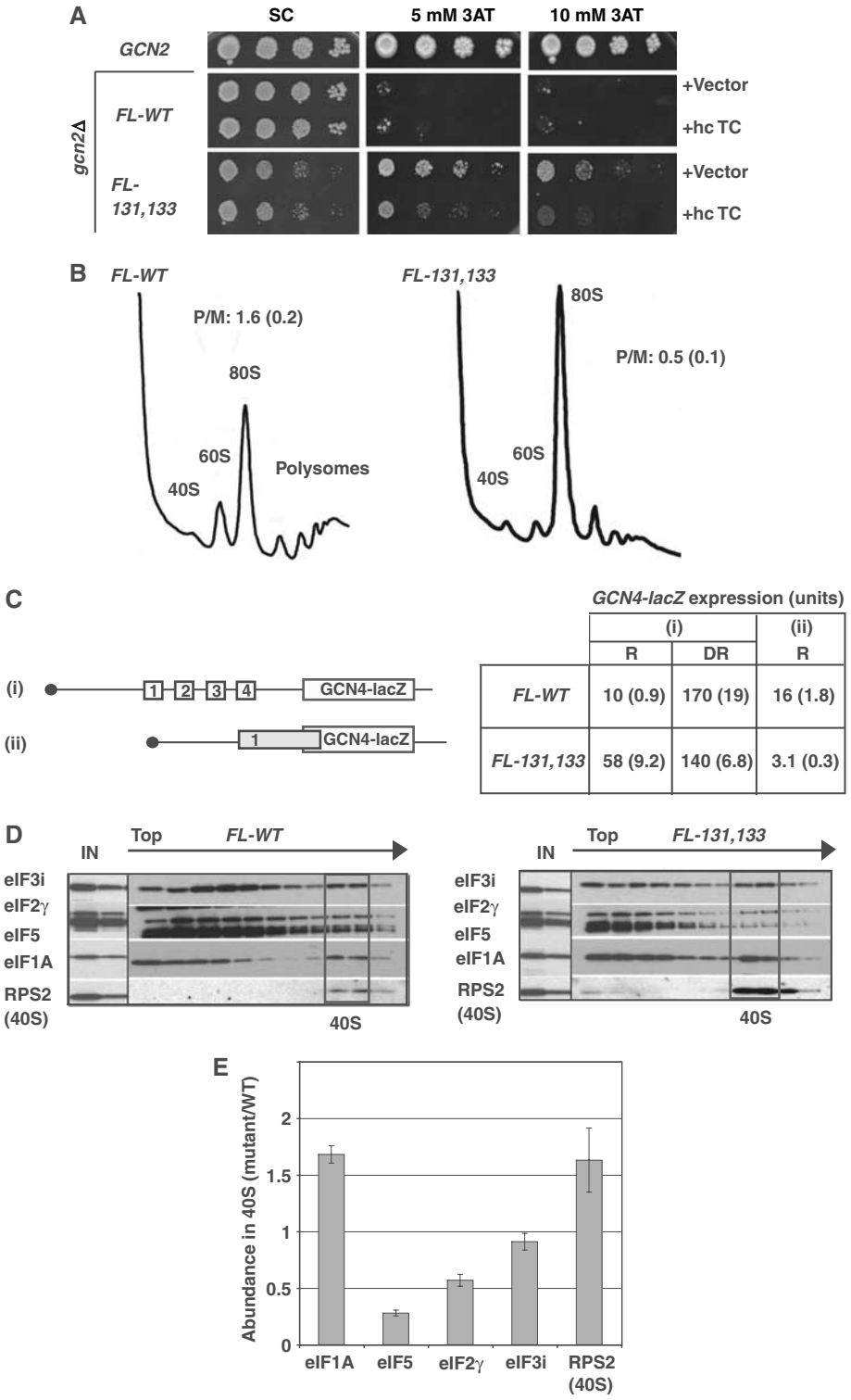

Figure 1 eIF1A CTT mutation *131,133* impairs *GCN4* translational control, translation initiation and PIC assembly *in vivo*. (**A**) Dilutions of *gcn2*Δ strains containing the FLAG-tagged wild-type (*FL-WT*) (strain H2999) or *131,133* mutant (*FL-131,133*) allele of *TIF11* (strain CFY615), plus empty vector or p1780-IMT (hc TC), together with an isogenic *GCN2* strain, were grown at 30°C on SC lacking uracil and leucine (SC-UL) for 3 days and SC-UL lacking histidine (SC-ULH) and containing 3-AT for 7 days. (**B**) Polysome profiles of H2999 and CFY615 cultured in SC-L and crosslinked with HCHO. WCEs were resolved by sedimentation through sucrose gradients and the gradients scanned at A_{254}. Polysome/monosome ratios (P/M, mean ± s.e., $n = 3$) are indicated. (**C**) *GCN2*$^+$ strains H3583 (*FL-WT*) and CFY217 (*FL-131,133*) harboring *GCN4-lacZ* reporter plasmids p180 or pM226, depicted in (i) and (ii), respectively, were grown in repressing (R) medium (SC-U) or derepressing (DR) medium (SC-U lacking Ile and Val and containing 0.5 μg/ml sulfometuron (SM) to inhibit Ile/Val biosynthesis) for 6 h. Units of β-galactosidase activity (nmol of *o*-nitrophenyl-β-D-galactopyranoside cleaved per minper mg) were assayed in WCEs of three replicate cultures and reported as means ± s.e. ($n = 6$). (**D**) Native PICs were measured in the strains described in (A) after crosslinking cells with HCHO and resolving WCEs by sedimentation through sucrose gradients. Fractions were subjected to Western analysis using the indicated antibodies, analyzing 1 and 0.2% aliquots of each input WCE (IN) in parallel. Fractions containing free 40S subunits are boxed. (**E**) Initiation factor binding to 40S subunits in three replicates of the experiment in (D) was quantified by calculating the ratios of the 40S signals in the mutant relative to the WT. Results are means ± s.e. ($n = 3$).

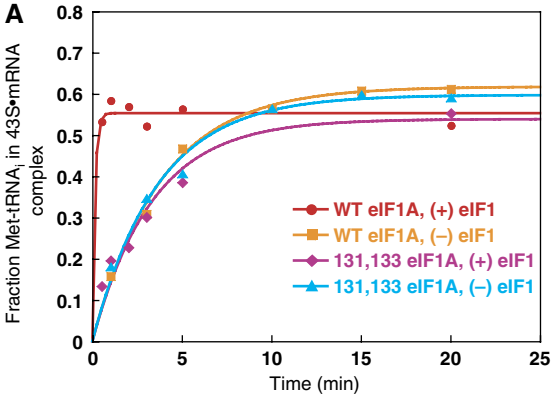

B

TC loading kinetics

eIF1A	k_{obs} (min^{-1})	
	–eIF1	+eIF1
WT	0.26±0.01	>2
131,133	0.30±0.14	0.31±0.07
7–11	0.09±0.04	>2

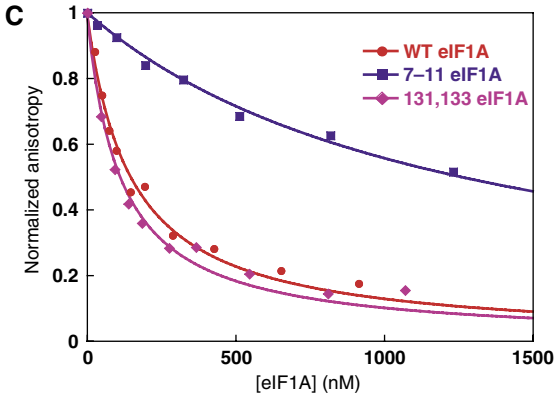

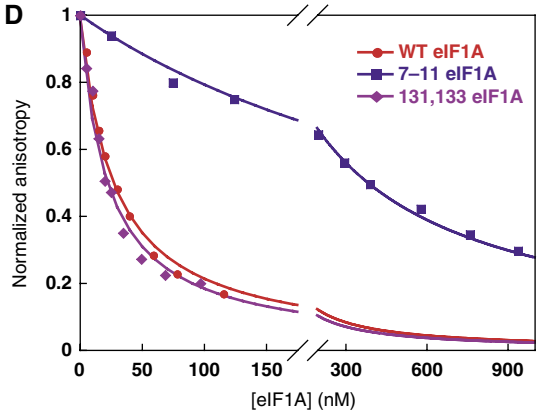

E

eIF1A binding to 40S

eIF1A	K_d (nM)		
	–eIF1	+eIF1	+ eIF1 +TC
WT	110±26	27.1±1.1	<1
131,133	80±12	22.5±1.3	<1
7–11	884±63	135±11	30±12
17–21	104±30	8.7±1.4	nd

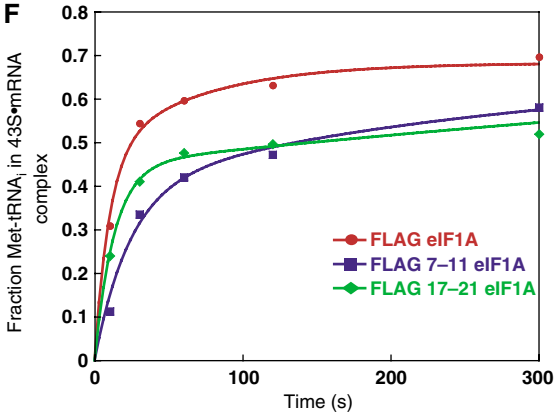

Figure 2 Effects of eIF1A mutations on kinetics of TC loading and 40S binding of eIF1A *in vitro*. (**A**) Preformed TC containing [^{35}S]-Met-tRNA$_i^{Met}$ was incubated with 40S subunits, eIF1, a model mRNA, and mutant or WT eIF1A, and the fraction of labeled [^{35}S]-Met-tRNA$_i^{Met}$ bound to 40S subunits was measured using a native gel assay. eIF1A was saturating (1 μM) in all cases. (**B**) Rate constants of 43S · mRNA complex formation measured as in (A). (**C**) Tetramethylrhodamine (TAMRA)-labeled WT eIF1A was prebound to 40S subunits and unlabeled mutant or WT eIF1A was added to compete with binding of labeled eIF1A. The decrease in fluorescence anisotropy of the labeled WT protein as a function of the concentration of unlabeled proteins yielded their K_d values. (**D**) Experiments as in (C) but with saturating eIF1 (1 μM). (**E**) K_d values for eIF1A binding to 40S subunits calculated from data in (C) and (D) in columns 2 and 3 and from experiments done with saturating preformed TC (0.9 μM) and eIF1 (1 μM) in column 4. (**F**) Mutations *7–11* and *17–21* reduce the rate of 43S · mRNA formation, measured in the presence of saturating eIF1, as in (A), when combined with the N-terminal FLAG tag. The *7–11* mutation reduces the rate constant to 1.3 min^{-1} from 3.5 min^{-1} for WT FL-eIF1A. Except in (F), eIF1A proteins lacked the FL tag.

and 12–16 were lethal and the 17–21 substitution conferred a Slg$^-$ phenotype, all without lowering the level of FL-eIF1A (Fekete *et al*, 2005). Interestingly, these phenotypes were suppressed by overexpressing WT eIF1 from a hc *SUI1* plasmid, whereas the Slg$^-$ phenotype of the CTT mutation *131,133* was exacerbated by hc *SUI1* (Figure 3A–B). The diminished polysome content of the *17–21* mutant was also partially suppressed by hc *SUI1* (Figure 3C), and *17–21* lowered the levels of eIF1, eIF5, eIF2, and eIF3 in the 40S fractions in a manner rescued by eIF1 overexpression (Figure 3D–E). The 40S binding of eIF1A itself was not diminished by the *17–21* mutation, and eIF1 overexpression led to a higher than WT level of 40S-bound 17–21 protein (Figure 3E). Thus, the *FL-17–21* mutation impairs PIC assembly by 40S-bound eIF1A in a manner rescued by increasing the eIF1 level in the cell.

The FL tag contributes to the phenotypes of the NTT mutations. In untagged *TIF11* or *TIF11-HA* (with a C-terminal HA_3 tag instead), the *17–21* mutation has no effect on growth; and *7–11* produces Slg$^-$, rather than lethality (that is not suppressed by hc *SUI1*) and does not reduce 40S binding of MFC components (data not shown). Thus, it appears that the NTT mutations strongly impair PIC assembly (in a manner rescued by eIF1) only when combined with the FL tag.

This last conclusion is consistent with results from *in vitro* analysis. Untagged 7–11 protein shows defects in 40S binding in the presence or absence of eIF1 and TC (Figure 2C–E). It also reduces the rate of TC loading in the absence of eIF1

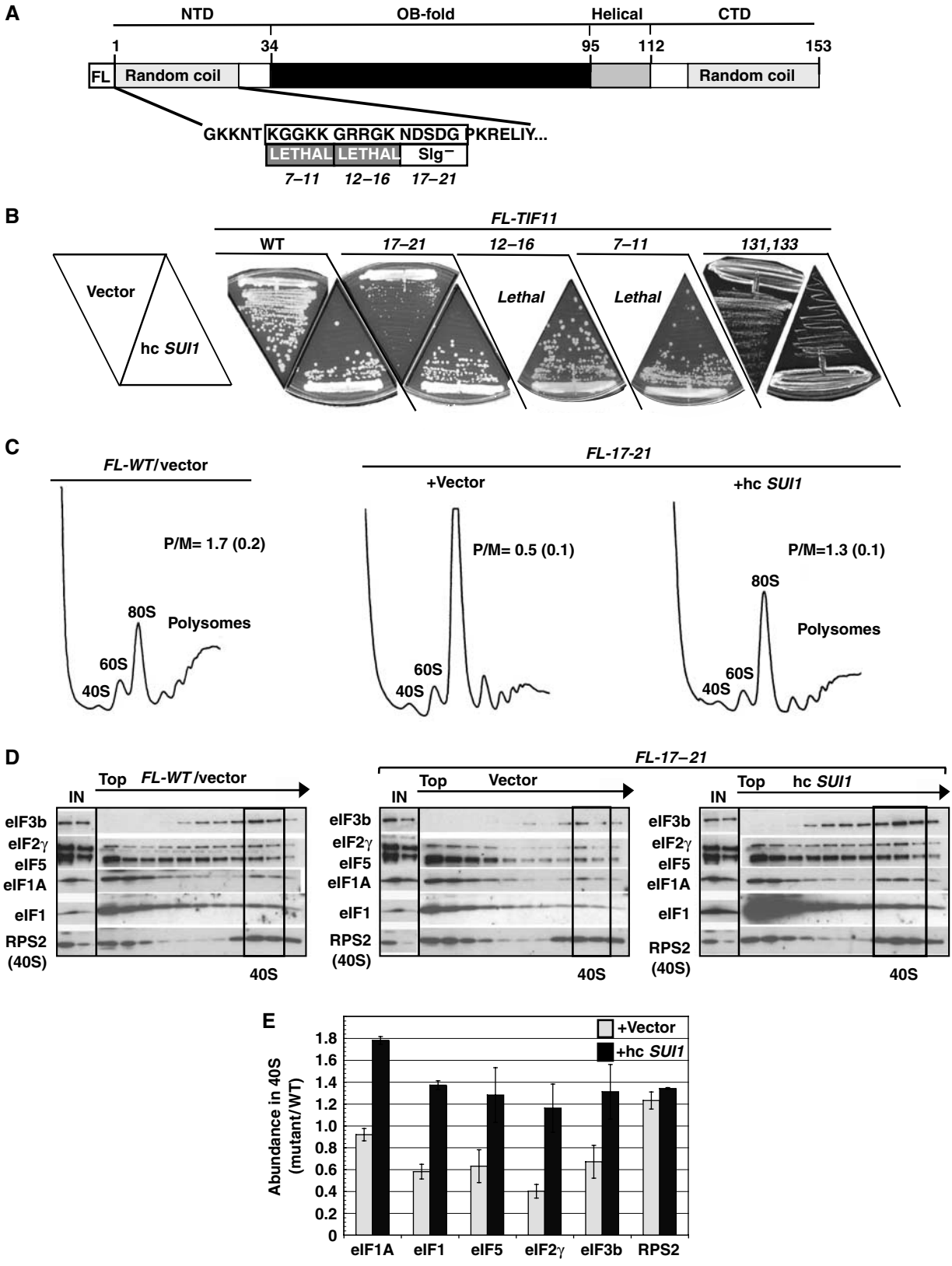

Figure 3 eIF1A NTT mutations reduce translation initiation and PIC levels in a manner suppressed by eIF1 overexpression. (**A**) Schematic of N-terminally FLAG-tagged eIF1A showing alanine-substituted NTT residues and corresponding growth phenotypes of three mutants. (**B**) *gcn2*Δ strains with the indicated *FL-TIF11* alleles and harboring hc *SUI1* plasmid YEp-SUI1-U (lower sectors) or empty vector (upper sectors) were grown on SC-UL medium at 30°C. (**C**) Polysome profiles of strains from (B) harboring *FL-WT* (H2999) or *FL-17–21* (CFY177) alleles of *TIF11* and empty vector or hc *SUI1*, measured as described in Figure 1B. (**D**) Native PICs in strains described in (C) measured as described in Figure 1D. (**E**) eIF binding to 40S subunits in three replicates of the experiment in (D) quantified by calculating the ratio of the 40S signal in the *FL-17–21* mutant, harboring empty vector or hc *SUI1* plasmid, relative to the WT strain. Results are means ± s.e. ($n = 3$).

when the mutant is supplied at a concentration high enough to compensate for its 40S binding defect (Figure 2B); however, there is no detectable defect in TC loading in the presence of eIF1 under these conditions (Figure 2B). Attaching FL to WT eIF1A reduces the rate of TC loading in the presence of eIF1 by ~30% (data not shown), and introducing the *17–21* or *7–11* mutations into FL-eIF1A reduces the rate further, with the *7–11* mutation having the greater effect (Figure 2F). eIF1 strongly stimulates the reaction rates for both of these eIF1A NTT mutants (data not shown).

These *in vitro* results coincide with our *in vivo* findings that combining *FL* with the *7–11* and *17–21* mutations produces additive defects in PIC assembly and growth that are suppressed by eIF1 overexpression. In addition to increasing the rate of TC loading, eIF1 overexpression also enhances 40S binding of the mutant eIF1As (Figures 2E and 3E) and other MFC components (Figure 3E), which probably contributes to suppression of the translation initiation defects in NTT mutants by excess eIF1 (Figure 3B and C). The residual Slg$^-$ phenotype of untagged *7–11* (which is not rescued by eIF1 overexpression) implies that this NTT mutation also disrupts a step downstream of PIC assembly, which fits with results below indicating that it impairs AUG recognition.

The 131,133 CTT mutation increases initiation at UUG codons in vivo

We have shown previously that the Δ*C* mutation in eIF1A confers increased initiation at a UUG triplet in *HIS4*, reducing the histidine auxotrophy (His$^-$ phenotype) produced by the absence of the AUG start codon in the *his4-303* allele (Sui$^-$ phenotype) (Fekete *et al*, 2005). We found that the *131,133* mutation also perturbs CTT function in start codon selection. First, *131,133* confers a marked increase in the expression of a *HIS4-lacZ* reporter containing a UUG start codon relative to that produced by a matched reporter containing an AUG (Figure 4A). Although we did not observe a His$^+$ phenotype in *131,133* cells harboring *his4-303*, this might be explained by the strong Slg$^-$ phenotype of this mutant. Supporting this interpretation, Western analysis of WT and *131,133* cells harboring an *myc*-tagged version of chromosomal *his4-303* revealed a ~nine-fold increase in the expression of myc-tagged his4-303 protein, with little change in *his4-303-myc* mRNA in the mutant cells (Figure 4B).

We also observed a decrease in leaky scanning of AUG start codons in the *131,133* mutant using a *GCN4-lacZ* reporter containing only an elongated version of uORF1 that overlaps the *GCN4* ORF. In WT cells, expression of this construct is very low because most ribosomes translate the elongated uORF1 and fail to reinitiate upstream at *GCN4* (Figure 1C, WT, construct ii). Interestingly, *131,133* conferred five-fold lower expression of this construct, suggesting diminished leaky scanning past the uORF1 AUG codon (Figure 1C, *131,133*, ii). It could be argued instead that *131,133* allows increased initiation at UUGs upstream of uORF1, but because translation of uORF1 is required for derepression, this should equally impair derepression of the WT *GCN4-lacZ* construct with all four uORFs, which was not observed (Figure 1C, *131,133*, i). A third indication that *131,133* alters AUG selection is that the mutation is synthetically lethal with the Sui$^-$ *SUI5* allele (data not shown), as observed previously on combining the *tif11-ΔC* mutation with *SUI5* (Fekete *et al*, 2005). We suggested previously that this synthetic lethality results from an additive effect of the mutations in elevating UUG selection, which reaches an intolerable level in the double mutant.

The eIF1A NTT mutations suppress utilization of UUG start codons in Sui$^-$ mutants

Remarkably, the eIF1A NTT mutations affect initiation at UUG triplets in a manner opposite to that of Sui$^-$ CTT mutations, suppressing the Sui$^-$ phenotypes conferred by *SUI5* and the eIF2β mutation *SUI3-2* (*SUI3-S264Y*). As expected (Huang *et al*, 1997), introducing plasmid-borne *SUI3-2* into the *TIF11-HA his4-303* strain confers a dominant His$^+$/Sui$^-$ phenotype and impairs growth on SC medium (Figure 4C, top two rows). The His$^+$ phenotype of *SUI3-2* was eliminated in strains containing the *7–11* or *17–21* mutations even though they grew better on SC medium than the corresponding WT *TIF11-HA* strain with *SUI3-2* (Figure 4C). Similarly, *17–21* and *7–11* suppressed the dominant His$^+$/Sui$^-$ phenotype of *SUI5* in *TIF11-HA* strains (Figure 4D, strains 1–3), and also when present in untagged *TIF11* (strains 4–6). The untagged *17–21* mutation also suppressed the Slg$^-$ phenotype of *SUI5* (Figure 4D, strains 4 and 6). Hence, the NTT mutations have Ssu$^-$ (Suppressor of Sui$^-$) phenotypes indicating reduced initiation at UUG codons in Sui$^-$ mutants.

Interestingly, attaching the FL tag to the N-terminus of eIF1A confers an Ssu$^-$ phenotype on its own, suppressing the strong Sui$^-$ phenotype of *SUI5* (Figure 4E, rows 6 and 9), whereas the C-HA$_3$ tag exacerbates the Sui$^-$ and Slg$^-$ phenotypes of *SUI3-2* (Figure 4E, rows 2 and 5) and the Slg$^-$ phenotype of *SUI5* (Figure 4E, rows 3 and 6). These opposite effects of the C-terminal and N-terminal tags reinforce the notion that altering the eIF1A CTT favors, whereas altering the NTT decreases, UUG selection in Sui$^-$ mutants.

The *FL-17–21* NTT mutation also affects leaky scanning in a manner opposite to that of CTT mutation *131,133*, producing 3.4-fold higher expression of the *GCN4-lacZ* reporter with elongated uORF1 (Figure 5A, iii). Leaky scanning of uORF1 in a construct containing all four WT uORFs should impair induction of *GCN4* because reinitiation after translation of uORF1 is required to bypass uORFs 3–4. In accordance with this possibility, *FL-17–21* decreases induction of the WT *GCN4-lacZ* reporter, reducing the induction ratio from 23 (observed in WT) to 12 (Figure 5A, i). Consistently, *FL-17–21* confers sensitivity to SM (SM^S) (Figure 5B, cf. rows 3 and 5), indicating a Gcn$^-$ phenotype, as also observed for *gcn2*Δ (Figure 5B, rows 1–2). Unlike *gcn2*Δ, however, the *FL-17–21* mutation does not decrease eIF2α phosphorylation in SM-induced cells (Figure 5C). The impaired derepression of *GCN4* cannot be attributed to reduced reinitiation following uORF1 translation because expression of a construct containing WT uORF1 as the sole uORF was unaffected by the *FL-17–21* mutation (Figure 5A, ii). The *7–11* mutation in the *TIF11-HA* background (where it is viable) also confers a strong SM^S phenotype (Figure 5B, rows 7 and 9). These data suggest that eIF1A NTT mutations impair *GCN4* translational control, at least partly, by allowing a fraction of PICs scanning from the cap to bypass the uORF1 AUG.

Whereas eIF1 overexpression suppresses the Slg$^-$ phenotype of the *FL-17–21* mutant, it does not suppress the SM^s/

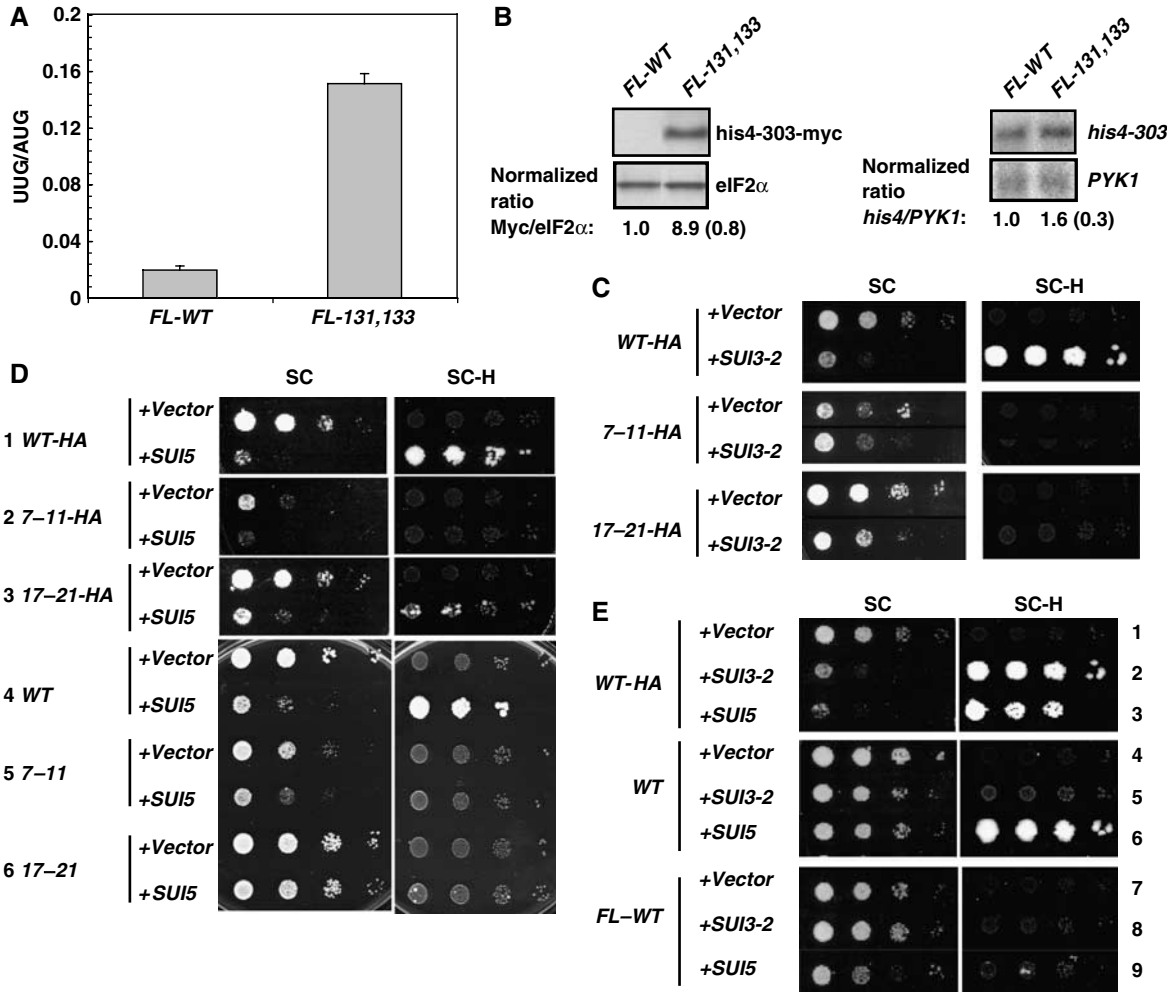

Figure 4 Opposite effects of eIF1A CTT and NTT mutations on initiation at UUG codons *in vivo*. (**A**) *his4-303* strains containing the *FL-WT* (H3583) or *FL-131,133* (CFY217) *TIF11* alleles and harboring *HIS4-lacZ* reporter plasmids with an AUG (p367) or UUG (p391) start codon grown in SC-U and assayed for β-galactosidase activity. Specific activities for three transformants were used to calculate the mean ± s.e. ratios ($n = 3$) for the UUG versus AUG reporter. (**B**) Cultures of *his4-303-myc* strains harboring *FL-WT* (CFY636) or *FL-131,133* (CFY798) alleles of *TIF11* were grown in SC-H. (*Left panel*) Western analysis of WCEs with antibodies against Myc epitope or eIF2α. Normalized ratios of Myc:eIF2α signals from three experiments are given as means ± s.e. ($n = 3$). Right panel: Northern analysis of *HIS4* and *PYK1* mRNAs. Normalized ratios of the *his4-303*:*PYK1* mRNA signals from three independent experiments are given as means ± s.e. ($n = 3$). (**C**) *TIF11* NTT mutations suppress the Slg$^-$ and Sui$^-$ phenotypes of *SUI3-2*. Serial dilutions of *his4-303* strains containing HA-tagged wild-type (*WT-HA*) (CFY840), *7–11-HA* (CFY842), or *17–21-HA* (CFY844) *TIF11* alleles harboring vector or *SUI3-2* plasmid pRSSUI3-S264Y-U were grown at 30°C on SC-U for 2 days and SC-UH for 7 days. (**D**) Growth on SC-U (2 days) and SC-UH (10 days) of *his4-303* strains containing *WT-HA*, *7–11-HA*, *17–21-HA*, or untagged wild-type (*WT*), *7–11* or *17–21* alleles of *TIF11*, harboring vector or *SUI5* plasmid YCpTIF5-G31R-U. (**E**) Growth on SC-U (2 days) and SC-UH (14 days) of HA-tagged (*WT-HA*), untagged (*WT*), or FLAG-tagged (*FL-WT*) wild-type alleles of *TIF11* carrying vector, *SUI3-2* plasmid pRSSUI3–264Y-U or *SUI5* plasmid YCpTIF5-G31R-U.

Gcn$^-$ phenotype of *FL-17–21* cells (Figure 5B, rows 5–6). These results fit with the idea that eIF1 overexpression overcomes the defect in PIC assembly (and attendant Slg$^-$ phenotype), but not the defect in start codon selection that contributes to the SM^S/Gcn$^-$ phenotype in *FL-17–21* cells.

Interestingly, *SUI3–2* eliminates the Slg$^-$ phenotype of *FL-17–21* (Figure 5D), reduces the increased leaky scanning conferred by *FL-17–21* (Figure 5E), and partially suppresses the SM^S/Gcn$^-$ phenotype in *FL-17–21* cells (data not shown). Thus, *FL-17–21* and *SUI3-2* mutually suppress their opposite effects on start codon selection. It is remarkable that *SUI5*, or introducing Δ*C* into the CTT, also suppresses the leaky scanning produced by *FL-17–21* (Figure 5F). Thus, the Sui$^-$ mutations *SUI3-2*, *SUI5*, and Δ*C*, which increase UUG initiation at *his4-303*, also increase recognition of the uORF1 AUG in the *FL-17–21* background, whereas *FL-17–21* reduces both initiation events. These data also support the notion that NTT (*FL-17–21*) and CTT (Δ*C*) mutations in eIF1A have opposite effects on AUG selection.

eIF1A mutations in the NTT and CTT have opposite effects on the stability of eIF1A interactions in reconstituted PICs

We considered the possibility that both the Ssu$^-$ and leaky scanning phenotypes of the eIF1A NTT mutations could arise from stabilization of an open, scanning conformation of the PIC, reducing the probability of initiation at either UUG or AUG codons. Our previous work indicates that eIF1A dissociates more slowly at AUG versus non-AUG codons, suggesting that tighter binding of eIF1A is a hallmark of the

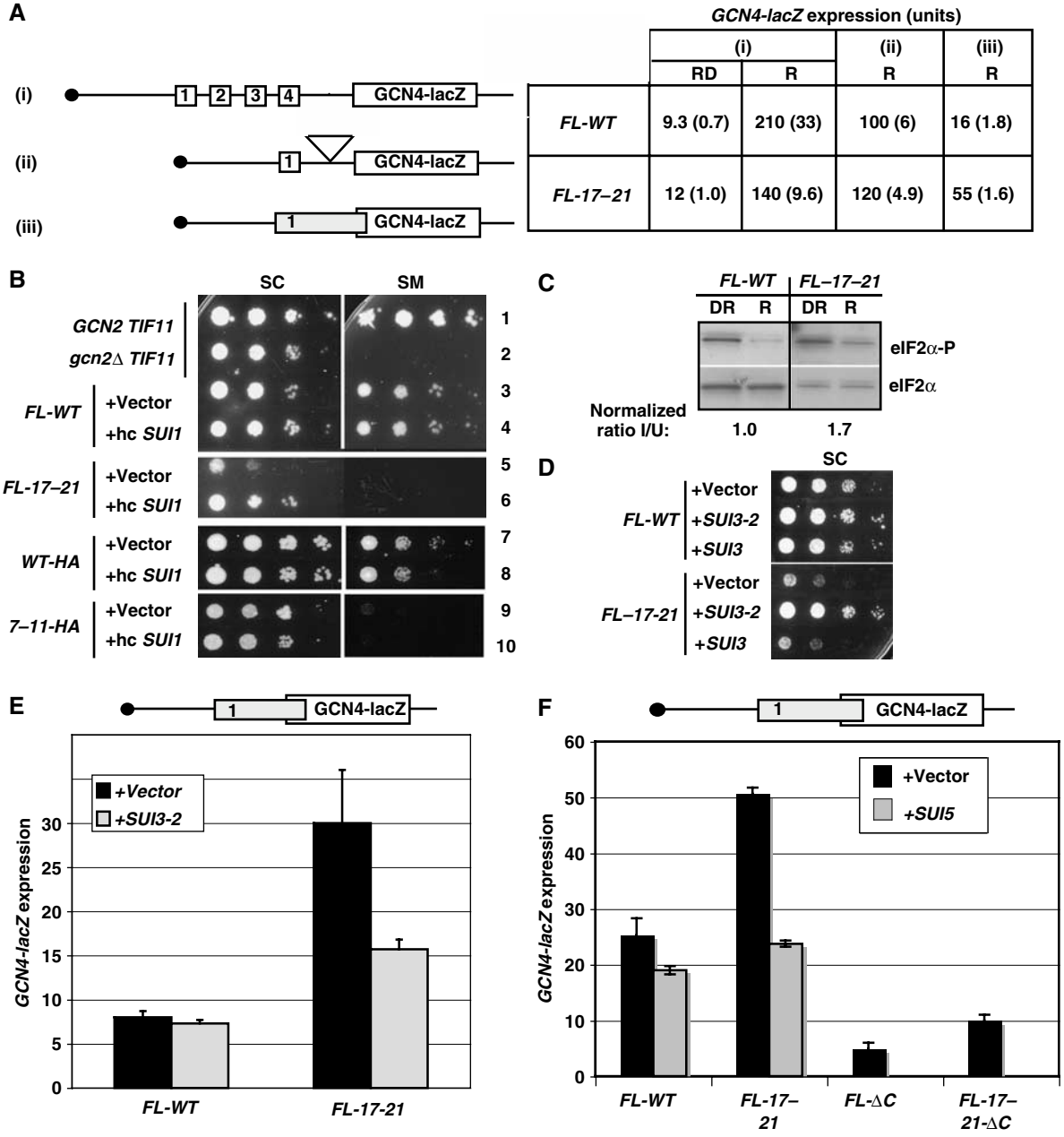

Figure 5 eIF1A NTT mutation *FL-17–21* confers leaky scanning and slow-growth phenotypes suppressed by *SUI3–2*. (**A**) *FL-17–21* impairs derepression of *GCN4* and increases leaky scanning of uORF1. *GCN2* strains containing *FL-WT* (H3583) or *FL-17–21* (CFY245) alleles of *TIF11* and *GCN4-lacZ* reporter plasmids p180, pM199, or pM226, depicted in (i), (ii), and (iii), respectively, were assayed in repressing and derepressing conditions as in Figure 1C. Units of specific activity are means ± s.e. ($n = 6$). (**B**) Growth on SC-UL or SC-ULIV + 0.5 μg/ml SM of *GCN2* strains containing *FL-WT*, *FL-17–21*, *WT-HA*, or *7–11-HA* alleles of *TIF11* and either vector or hc *SUI1* plasmid YEplac195-SUI1. Isogenic *GCN2* (H1642) and Δ*gcn2* (H1895) strains were analyzed as controls (top rows). (**C**) Western analysis of WCEs of *GCN2* strains containing *FL-WT* or *FL-17–21* alleles of *TIF11* described in (A) grown under repressing and derepressing conditions with antibodies specific for eIF2α phosphorylated on Ser-51 (eIF2α-P; upper panel) or total eIF2α (lower panel). Mean ratios of eIF2α-P/eIF2α were calculated and normalized to the WT ratio in each medium from two independent experiments. (**D**) Growth on SC-UL of *FL-WT* and *FL-17–21* strains described in (A) carrying vector, pRSSUI3-S264Y-U (*SUI3-2*), or p291 (*SUI3*). (**E**) *GCN2* strains containing *FL-WT* or *FL-17–21* alleles of *TIF11* and *GCN4-lacZ* reporter pM226 described in (A), and either vector or YCpSUI3-S264Y-W (*SUI3-2*), were assayed under repressing conditions as described in Figure 1C. Units of specific activity are means ± s.e. ($n = 6$). (**F**) Same as (E) except that *FL-WT* and *FL-17–21* strains harboring plasmid-borne *SUI5* and strains containing *FL-ΔC* or *FL-17–21-ΔC* alleles of *TIF11* and empty vector were analyzed.

closed, scanning-arrested IC formed at AUG (Maag *et al*, 2006). (Note that eIF1A dissociation in all cases is too slow to be physiologically relevant, but is a sensitive probe of the interactions between eIF1A and the PIC.) Accordingly, we asked whether the *FL-17–21* mutation increases the rate of eIF1A dissociation at both UUG and AUG complexes.

43S·mRNA(AUG) or 43S·mRNA(UUG) complexes were assembled with eIF1A, tagged at its C-terminus with fluorescein, in the presence of eIF5, chased with excess non-labeled eIF1A, and eIF1A dissociation was measured over time as the decrease in fluorescence anisotropy. WT eIF1A dissociates with biphasic kinetics, with rate constants for the

Table I Effects of eIF1A mutations on the kinetics of eIF1A dissociation from 43S.AUG and 43S.UUG PICs[a]

	eIF1A	eIF5		AUG	UUG
1	WT	WT	k_1	5.7±1.2	10.9±1.6
2			k_2	0.47±0.07	1.0±0.23
3			K_{amp}	5.5±0.7	4.0±0.88
4			*r* bound	0.205±0.004	0.185±0.007
5	WT	G31R	k_1	13.8±2.0	12±1.8
6			k_2	2.9±0.6	0.53±0.12
7			K_{amp}	1.3±0.6	5.8±2.8
8			*r* bound	0.187±0.005	0.206±0.007
9	FL-17–21	WT	k_1	8.8±1.3	13.5±0.5[b]
10			k_2	0.95±0.03	
11			K_{amp}	0.16±0.04	
12			*r* bound	0.184±0.003	0.171±0.0005
13	FL-17–21	G31R	k_1	34±1[b]	6.5±0[b]
14			k_2		
15			K_{amp}		
16			*r* bound	0.1530±0.0007	0.1726±0.0016
17	7–11	WT	k_1	17±2.5[b]	73±1[b]
18			k_2		
19			K_{amp}		
20			*r* bound	0.19±0.01	0.1808±0.0009
21	7–11	G31R	k_1	216±0[b]	28±2[b]
22			k_2		
23			K_{amp}		
24			*r* bound	0.1686±0.0002	0.1819±0.0039
25	131,133	WT	k_1	8.1±1.5	2.1±0.005[b]
26			k_2	0.315±0.015	
27			K_{amp}	4.7±0.2	
28			*r* bound	0.216±0.001	0.221±0.0001
29	131,133	G31R	k_1	10±0.65	7.8±1.2
30			k_2	2.3±0.65	0.49±0.01
31			K_{amp}	0.27±0.065	6.5±0.8
32			*r* bound	0.210±0.001	0.218±0.0025

All rates are $10^{-3}\,s^{-1}$.
[a]*r* bound is the fluorescence anisotropy of the labeled eIF1A in the 43S·mRNA complex.
[b]Single exponential.

fast and slow phases designated k_1 and k_2, respectively. K_{amp} is the ratio of the amplitudes of the slow to fast kinetic phases; hence values of $K_{amp}>1$ indicate that the slow phase dominates the reaction. When 40S binding of eIF1A is saturated (as here), the anisotropy (*r*) reflects the restriction of rotational motion of the eIF1A CTT in the complex, with higher *r* values indicating less freedom (Maag *et al*, 2006).

In accordance with earlier findings (Maag *et al*, 2006), the kinetics of eIF1A dissociation from AUG complexes in the presence of WT eIF5 is dominated by the slow phase (K_{amp} of 5.5; Table I, row 3), whereas replacing AUG with UUG reduces K_{amp} to 4.0 and increases k_1 and k_2, indicating weaker eIF1A binding. The CTT is also relatively less restricted (smaller *r* value) at UUG (Table I, rows 1–4, UUG). The *SUI5* mutation in eIF5 (G31R) decreases k_2 and increases *r* at UUG (Table I, rows 1–8), indicating tighter eIF1A binding at this near-cognate codon. Similar results were reported for the Sui$^-$ Δ*C* mutation in eIF1A (Maag *et al*, 2006). These findings allowed us to propose that tighter eIF1A binding to UUG complexes contributes to the increased initiation at UUG in these Sui$^-$ mutants. It is interesting that SUI5/G31R and Δ*C* both weaken eIF1A binding and increase rotational freedom of the CTT for AUG complexes (Table I, AUG) (Maag *et al*, 2006), suggesting that these mutations disfavor AUG recognition while increasing selection of UUG codons.

Dissociation of FL-17–21 from AUG complexes containing WT eIF5 showed a dramatic reduction in K_{amp} (Table I, AUG, rows 3 and 11) so that the rapid phase now dominates the reaction (see also kinetic data in Figure 6A). For the corresponding UUG complexes, the reaction is monophasic with a rate constant even higher than k_1 for WT complexes at UUG (Table I, UUG, rows 1 and 9). The CTT is also less restricted (smaller *r*) for both AUG and UUG complexes with FL-17–21. Similar conclusions hold for the double-mutant complexes formed with SUI5/G31R and FL-17–21 proteins, which exhibit rapid, monophasic dissociation and reduced *r* values for both AUG and UUG complexes, relative to those formed with SUI5/G31R and WT eIF1A (Table I, rows 13–16, and Figure 6A). The untagged 7–11 mutant also produced monophasic dissociation from AUG and UUG complexes at even higher rates and decreased *r* values (Table I, rows 17–24). Thus, the *FL-17–21* and *7–11* NTT mutations weaken eIF1A binding and increase mobility of the CTT in AUG and UUG

complexes in the presence of WT or SUI5/G31R forms of eIF5. These findings fit with the Ssu$^-$ and leaky scanning phenotypes of these eIF1A NTT mutations *in vivo*.

We also examined the untagged 131,133 CTT mutant to determine whether its Sui$^-$ phenotype involves tighter binding of eIF1A at UUG complexes. The 131,133 mutant clearly differs from WT in showing monophasic dissociation from the UUG complex, with a rate constant intermediate between the WT values of k_1 and k_2 for the UUG complex (Table I, row 25 versus rows 1–2). Comparing the monophasic rate constant for this mutant to a weighted-average rate constant for WT eIF1A suggests that the *131,133* mutation strengthens eIF1A binding at UUG in the presence (but not absence) of eIF5 (Figure 6B; last four bars), but has little effect on eIF1A dissociation from AUG complexes in the presence of WT eIF5 (Figure 6B, first four bars; Table I, rows 25–28 versus 1–4, AUG). The *131,133* mutation also decreases mobility of the CTT in complexes with UUG to the point where the anisotropy exceeds that seen for AUG with 131,133 or WT eIF1A (Table I, *r* values).

When combined with SUI5/G31R, the eIF1A-131,133 mutant slightly decreases the rate of dissociation at UUG, enhancing the tighter binding of eIF1A to UUG complexes produced by *SUI5*, and also exacerbates the effect of SUI5/G31R in weakening eIF1A interaction in AUG complexes. (Table I, rows 5–8 versus 29–32). A graph of K_{amp} for selected combinations of eIF1A and eIF5 proteins (Figure 6C) reveals that the combination of eIF1A-131,133 and SUI5/G31R reverses the normal effects of AUG and UUG on the rate of eIF1A dissociation. These biochemical data are consistent with the synthetic lethality of combining the *SUI5* and *131,133* mutations *in vivo*.

Discussion

In this paper, we provide new insights into the distinct roles of the unstructured tails of eIF1A in PIC assembly. The *131,133* CTT mutation lowers the level of native 43S PICs in extracts and derepresses *GCN4* translation in a manner partially suppressed by overexpressing TC. This mutation also decreases the rate of TC loading onto reconstituted PICs *in vitro*, consistent with its Gcd$^-$ phenotype. Ala substitutions of NTT residues 7–11, 12–16, or 17–21 in FL-tagged eIF1A conferred lethality or slow growth (for 17–21), and these phenotypes were suppressed by eIF1 overexpression. Overexpressing eIF1 also restored 40S association of MFC in *FL-17–21* cells. By contrast, eIF1 overproduction does not suppress the phenotypes of the CTT mutation *131,133* (Figure 3B) or of other (non-NTT) mutations we tested that impair native PIC assembly (data not shown).

In the presence of the N-terminal FL tag (which exacerbates NTT mutations), the *17–21* and *7–11* mutations decrease the rate of TC loading on reconstituted 48S PICs *in vitro*. The untagged 7–11 mutant is also defective for this function in the absence of eIF1, but is not detectably different from WT in the presence of eIF1. Thus, the *7–11* substitutions reduce the rate of TC loading in a manner overcome by eIF1. By contrast, the CTT mutation *131,133* impairs TC loading only in the presence of eIF1. Clearly, mutations in the unstructured NTT and CTT impair PIC assembly by different mechanisms.

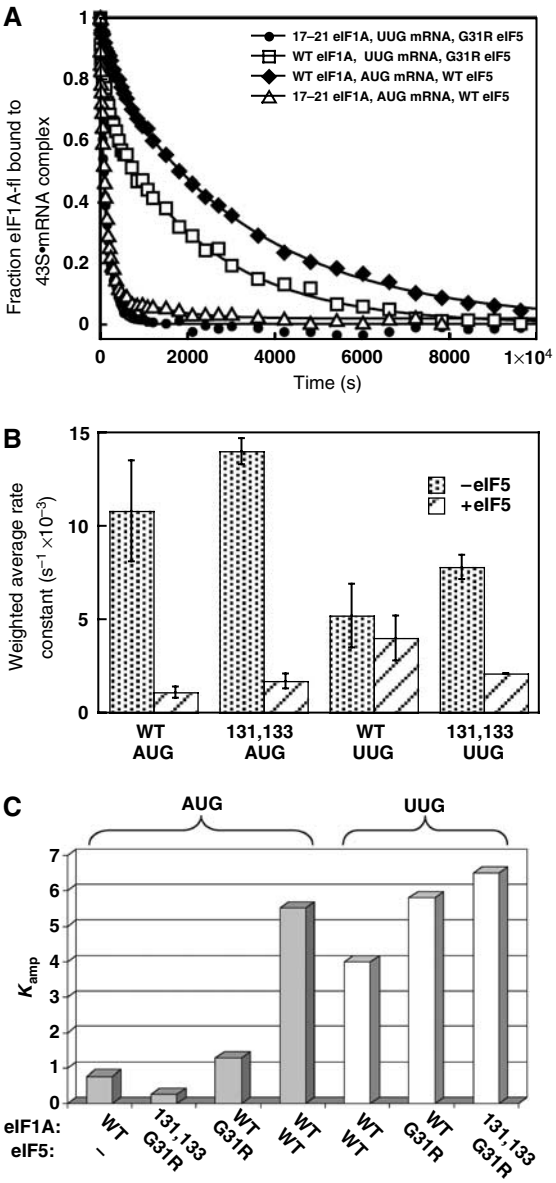

Figure 6 Sui$^-$ and Ssu$^-$ mutations in eIF1A affect the rate of eIF1A dissociation from reconstituted 48S PICs. (**A**) The *FL-17–21* mutation accelerates eIF1A dissociation from 43S·mRNA(AUG) complexes in the presence of WT eIF5 and from 43S·mRNA(UUG) complexes in the presence of eIF5-G31R. Dissociation of fluorescein-conjugated FL-tagged mutant or untagged WT eIF1A was monitored by anisotropy changes when chased from the 43S·mRNA·eIF5 complex with unlabeled eIF1A. (**B**) Weighted-average rate constants calculated from data in Table I by multiplying the rate constant of each phase by the amplitude of that phase and summing the resulting numbers. Weighted rate constants are misleading when there is a very fast phase with a small amplitude, but this is not the case in comparisons made here. (**C**) Plot of selected K_{amp} values from Table I for the indicated combinations of untagged eIF1A (WT or *131,133* mutant) and eIF5 (WT or G31R mutant) proteins.

One way to explain suppression of the eIF1A NTT mutations by eIF1 overexpression is to propose that they disrupt a function of eIF1A in recruiting TC and other MFC components that is redundant with eIF1 activity. Consistent with this, eIF1A can bind to eIF2 and eIF3, and their interactions in the PIC require the eIF1A NTT (Olsen *et al*, 2003). eIF1 interacts with eIF2β, eIF3c, and eIF5 and is critical for MFC association with 40S subunits *in vivo* (Asano *et al*, 2001a;

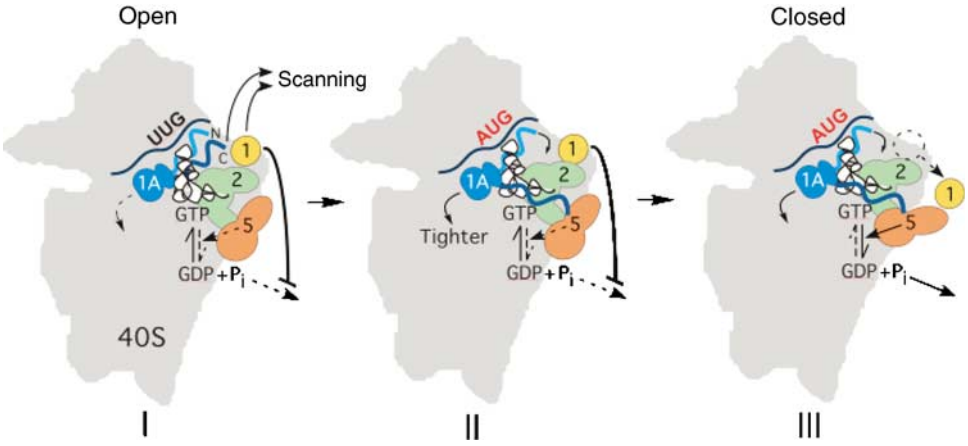

Figure 7 Hypothetical model for functions of eIF1A and eIF1 in scanning and AUG selection. (I) 48S PIC in the open, scanning-conducive conformation with a non-AUG in the P-site and the β-barrel fold of eIF1A occupying the A-site. GTP in the TC is partially hydrolyzed in a manner stimulated by eIF5, but P_i release from eIF2-GDP-P_i is blocked by eIF1 bound near the P-site. The CTT of eIF1A (dark-blue wavy line) is in proximity to eIF1 and both factors promote scanning. (II) Pairing of the anticodon of Met-$tRNA_i^{Met}$ with AUG in the P-site elicits a rapid conformational change that increases the distance between eIF1A-CTT and eIF1 and results in tighter binding of eIF1A to the IC. eIF1A–IC interaction is weakened by eIF1A-CTT, which in turn is antagonized by eIF5 (perhaps through direct CTT–eIF5 interaction as suggested here) to strengthen eIF1A-IC association. The eIF1A NTT (light blue wavy line) also strengthens eIF1A–IC interaction. Hence, eIF1A–CTT mutations favor the closed complex, allowing increased initiation at UUG (Sui$^-$ phenotype), whereas NTT mutations favor the open complex, suppressing initiation at UUG (Ssu$^-$ phenotype). (III) Dissociation of eIF1 from its location near the P-site allows release of P_i from eIF2-GDP-Pi, an irreversible step that drives GTP hydrolysis to completion and finalizes start codon selection.

Singh *et al*, 2004), and eIF1 binds directly to the 40S (Lomakin *et al*, 2000). Hence, overexpressing eIF1 could drive 40S–MFC interactions and compensate for a reduced ability of eIF1A NTT mutants to promote MFC recruitment. In addition, binding of eIF1A and eIF1 to the 40S subunit is thermodynamically coupled (Maag and Lorsch, 2003; Majumdar *et al*, 2003), and overexpression of eIF1 increases 40S binding of the *FL-17–21* protein *in vivo* (Figure 3E). This effect may contribute to suppressing the growth defect of this mutant, and also the lethality of the *FL-7–11* mutation, considering that *7–11* confers a marked 40S binding defect *in vitro* (Figure 2E).

To explain why the CTT mutation *131,133* impairs TC loading *in vitro* only in the presence of eIF1, it could be proposed that *131,133* eliminates a functional interaction between eIF1A and eIF1 required for the stimulatory effect of eIF1 on TC loading. This would be another instance of their interdependence in PIC assembly revealed previously by the thermodynamic coupling of their 40S binding (Maag and Lorsch, 2003; Majumdar *et al*, 2003), which is not disrupted by the *131,133* mutation. The fact that *131,133* more seriously impedes TC loading in the presence versus absence of mRNA could indicate that it also impairs the ability of mRNA to stimulate TC loading in the reconstituted system (Maag *et al*, 2005).

The Δ*C* and *131,133* CTT mutations confer Sui$^-$ phenotypes *in vivo*, and the C-terminal HA_3 tag on WT eIF1A exacerbates the Sui$^-$ phenotype of eIF2β mutation *SUI3–2*. Thus, altering the eIF1A CTT enhances initiation at UUG. Remarkably, the *7–11* and *17–21* substitutions in the NTT, and also the N-terminal FL tag, have the opposite effect and suppress the Sui$^-$ phenotypes of mutations in eIF2β or eIF5. The CTT and NTT eIF1A mutations also have opposing effects on AUG selection, with CTT mutations decreasing and NTT mutations increasing leaky scanning of the *GCN4* uORF1 AUG codon. Remarkably, the CTT mutation Δ*C*, and other Sui$^-$ mutations (*SUI3-2* and *SUI5*) suppress the increased leaky scanning phenotype of *FL-17–21*. Thus, the CTT mutations enhance UUG and AUG selection, while the NTT mutations suppress both events.

The increased leaky scanning of uORF1 in the NTT mutants likely contributes to their impaired ability to derepress translation of *GCN4* (Gcn$^-$ phenotype) when all four uORFs are present, as uORF1 translation is required for the subsequent bypass of uORFs 2–4 by reinitiating 40S subunits when TC levels are reduced. This defect can help explain why the *FL-17–21* NTT mutation does not produce a Gcd$^-$ phenotype (derepression of *GCN4* in non-starvation conditions) despite a reduced rate of TC loading on 40S subunits and decreased PIC levels *in vivo*, as observed previously for eIF5 mutations (Singh *et al*, 2005).

Our recent *in vitro* analysis of eIF1A interactions with reconstituted 48S complexes revealed that AUG in the P-site and eIF5 collaborate to produce tighter binding of eIF1A. Moreover, the Δ*C* and *SUI5* Sui$^-$ mutations tighten eIF1A binding to complexes with UUG start codons, but weaken binding to AUG complexes. This led us to propose that eIF1A binds less tightly to the open, scanning-conducive conformation of the PIC than to the closed, scanning-incompetent conformation of the IC at AUG (see model in Figure 7). The fast and slow phases of eIF1A dissociation would reflect the different affinities of eIF1A for open and closed conformations, which exist in equilibrium (Maag *et al*, 2006). (It could also be proposed that eIF1A does not dissociate from the closed complex and the slow phase reflects the transition from closed to open conformation. The probability of shifting from closed to open conformation, favored at UUG and disfavored at AUG, would then dictate the fast and slow rates of eIF1A dissociation, respectively, from these two complexes.)

The new Sui$^-$ mutation *131,133* strengthens eIF1A binding and restricts motion of the CTT in UUG complexes, consistent with the idea that it promotes a closed conformation at non-AUGs. Strikingly, the Ssu$^-$ eIF1A NTT mutations *FL-17–21*

and *7–11* have the opposite effects in UUG complexes with either WT or G31R/SUI5 forms of eIF5. These results help explain why NTT mutations suppress initiation at UUG in Sui$^-$ mutants and they support our model that tighter binding of eIF1A to the IC is an important step in start site selection (Figure 7). The *FL-17–21* and *7–11* mutations also weaken eIF1A binding to AUG complexes, which fits with the increased leaky scanning of the uORF1 AUG codon in *FL-17–21* cells. The fact that the Sui$^-$ mutations *SUI3-2*, *SUI5*, and Δ*C* (in eIF1A itself) diminish this leaky scanning phenotype suggest that they stimulate the transition from open to closed conformations with either AUG or UUG in the P-site.

Two aspects of the eIF1A dissociation data are at odds with the *in vivo* results. The Sui$^-$ mutations *SUI5* and Δ*C* weaken eIF1A binding at AUG complexes while strengthening eIF1A binding to non-AUG complexes (Maag *et al*, 2006) (Table I), and the CTT mutation *131,133* exacerbates both trends. This suggests that these Sui$^-$ mutations disfavor the closed conformation at AUG while enhancing the closed conformation at UUG. Indeed, on the basis of eIF1A dissociation rates (and anisotropy values), one would predict a higher rate of initiation at UUG versus AUG in the *SUI5* and Δ*C* mutants, which is not observed. One would also predict that these mutations increase leaky scanning of the uORF1 AUG, whereas *131,133* and Δ*C* decrease leaky scanning in otherwise WT cells, and *SUI5* and Δ*C* suppress this phenotype in *FL-17–21* cells. These discrepancies suggest that the altered eIF1A affinity for the initiation complex, and the underlying conformational change, involves only one step in the transition to the closed, scanning-arrested IC from the scanning PIC (Figure 7).

We suggest that this transition includes several conformational changes in the 40S subunit that restrict the mRNA binding channel or strengthen interactions of TC with mRNA to impede scanning, make the P-site more accommodating to Met-tRNA$_i^{Met}$, or enhance the ability of eIF5 to stimulate GTP hydrolysis or P_i release from eIF2-GDP-Pi. eIF1 has been implicated in opposing many of these steps as a negative effector of non-AUG selection (Pestova and Kolupaeva, 2002; Unbehaun *et al*, 2004; Valasek *et al*, 2004; Algire *et al*, 2005), and eIF1 dissociation is thought to be required for AUG selection (Maag *et al*, 2006). These different steps may combine additively or synergistically to account for the ~30-fold difference between initiation rates at AUG versus UUG observed *in vivo*. By overcoming the inhibitory effect of eIF1 on these other steps, AUG in the P-site may override the effects of *SUI5* and Δ*C* in weakening eIF1A binding to AUG complexes. In fact, as these mutations produce Sui$^-$ phenotypes, they likely stimulate the additional steps that promote scanning arrest, GTP hydrolysis, and P_i release, neutralizing the inhibitory effects on the eIF1A-related conformational change at AUG. This could explain why UUG initiation remains lower than AUG initiation in *SUI5*, Δ*C*, and *131,133* mutants, and also why *SUI5*, Δ*C*, and *131,133* decrease, rather than increase, leaky scanning at uORF1.

It is also noteworthy that the eIF1A NTT mutations (especially *7–11*) evoke a stronger reduction in eIF1A affinity for AUG complexes than the *SUI5*, *ΔC*, and *131,133* mutations. In addition, their suppression of Sui$^-$ phenotypes suggests that NTT mutations may inhibit one of the other steps leading to IC formation that the Sui$^-$ mutations likely stimulate in order to enhance UUG initiation. In fact, we found recently that the NTT mutation *FL-17–21* slows down both the conformational change that increases eIF1A–eIF1 separation and the dissociation of eIF1 from its 40S binding site upon AUG recognition (unpublished observations). We propose that the cumulative effect of multiple impediments to IC formation at a start codon caused by *FL-17–21* accounts for its increased leaky scanning of AUGs.

It could be argued that if our reconstituted system displayed the proper selectivity, then 43S·mRNA(UUG) complexes would be too unstable for measurements of eIF1A dissociation at the rates we observe ($\sim$5–50 h^{-1}). It is possible that we are missing in our system a selectivity factor that destabilizes non-AUG complexes (e.g. eIF4G). However, it is also possible that the UUG complexes are dynamic and slide along the mRNA, but that UUG is highly favored over the other triplets for P-site occupancy, so that the dissociation reaction involves an ensemble of different complexes that is heavily dominated by the UUG complex. Indeed, we have evidence from TC-binding data that the UUG complex is more stable than nearly all other non-AUG complexes, whereas less stable than the AUG complex (unpublished observations). Moreover, the fact that Sui$^-$ and Ssu$^-$ mutations in eIF1A have opposite effects on the kinetics of eIF1A dissociation from UUG complexes clearly indicates that the reconstituted system recapitulates at least some critical elements governing AUG selectivity *in vivo*.

Finally, it is notable that the entire set of phenotypes exhibited by the eIF1A NTT mutations described above are displayed by the *DGNK$_{53-56}$AANA* mutation (Fekete *et al*, 2005) in conserved surface residues of the β-barrel. The *53–56* mutation impairs initiation and reduces native PIC levels in a manner diminished by hc *SUI1*, suppresses the Sui$^-$ phenotype of *SUI5* (Ssu$^-$), increases leaky scanning of uORF1 and impairs derepression of *GCN4* (Gcn$^-$), and its Gcn$^-$ and Slg$^-$ phenotypes are partially suppressed by *SUI3-2* (Supplementary Figures S2–S3). Thus, this region of the β-barrel surface (between β strands 2–3) (Battiste *et al*, 2000) may cooperate with the NTT in PIC assembly and regulating AUG selection.

Materials and methods

Plasmids and yeast strains used are listed in Tables II and III of Supplementary data along with descriptions of their constructions and all relevant biochemical methods.

Supplementary data

Supplementary data are available at *The EMBO Journal* Online (http://www.embojournal.org).

Acknowledgements

We thank Tom Dever and our laboratories for helpful suggestions, Stephen Blakely and Azadeh Esmaeli for technical assistance, Ernie Hannig, Tom Donahue, Jon Warner, and Fan Zhang for antibodies or strains. This work was supported in part by the Intramural Research Program of the NICHD, NIH.

References

Algire MA, Maag D, Lorsch JR (2005) P_i release from eIF2, not GTP hydrolysis, is the step controlled by start-site selection during eukaryotic translation initiation. *Mol Cell* **20:** 251–262

Algire MA, Maag D, Savio P, Acker MG, Tarun Jr SZ, Sachs AB, Asano K, Nielsen KH, Olsen DS, Phan L, Hinnebusch AG, Lorsch JR (2002) Development and characterization of a reconstituted yeast translation initiation system. *RNA* **8:** 382–397

Asano K, Phan L, Valasek L, Schoenfeld LW, Shalev A, Clayton J, Nielsen K, Donahue TF, Hinnebusch AG (2001a) A multifactor complex of eIF1, eIF2, eIF3, eIF5, and tRNA(i)Met promotes initiation complex assembly and couples GTP hydrolysis to AUG recognition. *Cold Spring Harb Symp Quant Biol* **66:** 403–415

Asano K, Shalev A, Phan L, Nielsen K, Clayton J, Valášek L, Donahue TF, Hinnebusch AG (2001b) Multiple roles for the carboxyl terminal domain of eIF5 in translation initiation complex assembly and GTPase activation. *EMBO J* **20:** 2326–2337

Battiste JB, Pestova TV, Hellen CUT, Wagner G (2000) The eIF1A solution structure reveals a large RNA-binding surface important for scanning function. *Mol Cell* **5:** 109–119

Donahue T (2000) Genetic approaches to translation initiation in *Saccharomyces cerevisiae*. In *Translational Control of Gene Expression*, Sonenberg N, Hershey JWB, Mathews MB (eds), pp 487–502. Cold Spring Harbor: Cold Spring Harbor Laboratory Press

Fekete CA, Applefield DJ, Blakely SA, Shirokikh N, Pestova T, Lorsch JR, Hinnebusch AG (2005) The eIF1A C-terminal domain promotes initiation complex assembly, scanning and AUG selection *in vivo*. *EMBO J* **24:** 3588–3601

Hershey JWB, Merrick WC (2000) Pathway and mechanism of initiation of protein synthesis. In *Translational Control of Gene Expression*, Sonenberg N, Hershey JWB, Mathews MB (eds), pp 33–88. Cold Spring Harbor: Cold Spring Harbor Laboratory Press

Hinnebusch AG (2000) Mechanism and regulation of initiator methionyl-tRNA binding to ribosomes. In *Translational Control of Gene Expression*, Sonenberg N, Hershey JWB, Mathews MB (eds), pp 185–243. Cold Spring Harbor: Cold Spring Harbor Laboratory Press

Hinnebusch AG (2005) Translational regulation of gcn4 and the general amino acid control of yeast. *Annu Rev Microbiol* **59:** 407–450

Huang H, Yoon H, Hannig EM, Donahue TF (1997) GTP hydrolysis controls stringent selection of the AUG start codon during translation initiation in *Saccharomyces cerevisiae*. *Genes Dev* **11:** 2396–2413

Jivotovskaya AV, Valasek L, Hinnebusch AG, Nielsen KH (2006) Eukaryotic translation initiation factor 3 (eIF3) and eIF2 can promote mRNA binding to 40S subunits independently of eIF4G in yeast. *Mol Cell Biol* **26:** 1355–1372

Kolupaeva VG, Unbehaun A, Lomakin IB, Hellen CU, Pestova TV (2005) Binding of eukaryotic initiation factor 3 to ribosomal 40S subunits and its role in ribosomal dissociation and anti-association. *RNA* **11:** 470–486

Lomakin IB, Hellen CU, Pestova TV (2000) Physical association of eukaryotic initiation factor 4G (eIF4G) with eIF4A strongly enhances binding of eIF4G to the internal ribosomal entry site of encephalomyocarditis virus and is required for internal initiation of translation. *Mol Cell Biol* **20:** 6019–6029

Lomakin IB, Kolupaeva VG, Marintchev A, Wagner G, Pestova TV (2003) Position of eukaryotic initiation factor eIF1 on the 40S ribosomal subunit determined by directed hydroxyl radical probing. *Genes Dev* **17:** 2786–2797

Maag D, Algire MA, Lorsch JR (2006) Communication between eukaryotic translation initiation factors 5 and 1A within the ribosomal pre-initiation complex plays a role in start site selection. *J Mol Biol* **356:** 724–737

Maag D, Fekete CA, Gryczynski Z, Lorsch JR (2005) A conformational change in the eukaryotic translation preinitiation complex and release of eIF1 signal recognition of the start codon. *Mol Cell* **17:** 265–275

Maag D, Lorsch JR (2003) Communication between eukaryotic translation initiation factors 1 and 1A on the yeast small ribosomal subunit. *J Mol Biol* **330:** 917–924

Majumdar R, Bandyopadhyay A, Maitra U (2003) Mammalian translation initiation factor eIF1 functions with eIF1A and eIF3 in the formation of a stable 40 S preinitiation complex. *J Biol Chem* **278:** 6580–6587

Olsen DS, Savner EM, Mathew A, Zhang F, Krishnamoorthy T, Phan L, Hinnebusch AG (2003) Domains of eIF1A that mediate binding to eIF2, eIF3 and eIF5B and promote ternary complex recruitment *in vivo*. *EMBO J* **22:** 193–204

Pestova TV, Borukhov SI, Hellen CUT (1998) Eukaryotic ribosomes require initiation factors 1 and 1A to locate initiation codons. *Nature* **394:** 854–859

Pestova TV, Kolupaeva VG (2002) The roles of individual eukaryotic translation initiation factors in ribosomal scanning and initiation codon selection. *Genes Dev* **16:** 2906–2922

Singh CR, Curtis C, Yamamoto Y, Hall NS, Kruse DS, He H, Hannig EM, Asano K (2005) Eukaryotic translation initiation factor 5 is critical for integrity of the scanning preinitiation complex and accurate control of GCN4 translation. *Mol Cell Biol* **25:** 5480–5491

Singh CR, He H, Ii M, Yamamoto Y, Asano K (2004) Efficient incorporation of eukaryotic initiation factor 1 into the multifactor complex is critical for formation of functional ribosomal preinitiation complexes *in vivo*. *J Biol Chem* **279:** 31910–31920

Unbehaun A, Borukhov SI, Hellen CU, Pestova TV (2004) Release of initiation factors from 48S complexes during ribosomal subunit joining and the link between establishment of codon-anticodon base-pairing and hydrolysis of eIF2-bound GTP. *Genes Dev* **18:** 3078–3093

Valášek L, Nielsen KH, Hinnebusch AG (2002) Direct eIF2-eIF3 contact in the multifactor complex is important for translation initiation *in vivo*. *EMBO J* **21:** 5886–5898

Valasek L, Nielsen KH, Zhang F, Fekete CA, Hinnebusch AG (2004) Interactions of eukaryotic translation initiation factor 3 (eIF3) subunit NIP1/c with eIF1 and eIF5 promote preinitiation complex assembly and regulate start codon selection. *Mol Cell Biol* **24:** 9437–9455

